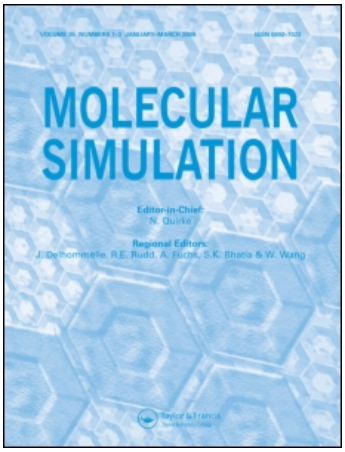

Molecular Simulation
Publication details, including instructions for authors and subscription information:
http://www.informaworld.com/smpp/title~content=t713644482

Direct Evaluation of Solid-Liquid Equilibria by Molecular Dynamics Using Gibbs-Duhem Integration

Martin Lísal[a]; Václav Vacek[b]
[a] E. Hála Laboratory of Thermodynamics, Institute ofChemical Process Fundamentals, Academy of Sciences, Prague, Czech Republic [b] Department of Physics, Czech Technical University, Prague, Czech Republic

To cite this Article Lísal, Martin and Vacek, Václav(1997) 'Direct Evaluation of Solid-Liquid Equilibria by Molecular Dynamics Using Gibbs-Duhem Integration', Molecular Simulation, 19: 1, 43 — 61
To link to this Article: DOI: 10.1080/08927029708024137
URL: http://dx.doi.org/10.1080/08927029708024137

Molecular Simulation, 1997, Vol. 19, pp. 43–61
Reprints available directly from the publisher
Photocopying permitted by license only

DIRECT EVALUATION OF SOLID–LIQUID EQUILIBRIA BY MOLECULAR DYNAMICS USING GIBBS-DUHEM INTEGRATION

MARTIN LÍSAL[a] and VÁCLAV VACEK[b]

[a]*E. Hála Laboratory of Thermodynamics, Institute of Chemical Process Fundamentals, Academy of Sciences, 165 02 Prague 6, Czech Republic;*
[b]*Department of Physics, Czech Technical University, 167 06 Prague 6, Czech Republic*

(Received November 1996; accepted November 1996)

An application of the Gibbs-Duhem integration [D. A. Kofke, *J. Chem. Phys.*, **98**, 4149 (1993)] for the direct evaluation of solid–liquid equilibria by molecular dynamics is presented. The Gibbs-Duhem integration combines the best elements of the Gibbs ensemble Monte Carlo technique and thermodynamic integration. Given conditions of coexistence at one coexistence point, simultaneous but independent constant pressure–constant temperature molecular dynamics simulations of each phase are carried out in succession along saturation lines. In each simulation, the saturated pressure is adjusted to satisfy the Clapeyron equation, a first-order nonlinear differential equation that prescribes how the pressure must change with the temperature to maintain coexistence. The Clapeyron equation is solved by the predictor–corrector method. Running averages of enthalpy and density of each phase are used to evaluate the right-hand side of the Clapeyron equation. The Gibbs-Duhem integration method is applied to a two-centre Lennard-Jones system with elongation 0.67. The starting coexistence point is determined as the point of intersection of solid and liquid isotherm branches in the pressure *vs* chemical potential plane.

Keywords: Solid–liquid equilibria; Gibbs-Duhem Integration; Clapeyron equation

1 INTRODUCTION

Prediction of solid–liquid equilibria (SLE) by thermodynamic integration is tedious and time-consuming work. It involves calculation of the equation of state and free energy for liquids and solids at temperatures of interest [1–3]. Then, a solid–liquid coexistence point is obtained as the point of intersection of solid and liquid isotherm branches in the pressure *vs* chemical potential plane [4].

In principle, the Gibbs ensemble Monte Carlo (GEMC) technique [5] can also be applied to SLE. However, at high densities, the particle transfer step in the GEMC method has a very low probability of acceptance [6]. Hence, practical application of the GEMC technique to SLE seems problematic or even impossible.

Recently, Kofke [7] has proposed a new method for the direct evaluation of phase coexistence by molecular simulations: the Gibbs-Duhem integration. He applied it to vapour–liquid equilibria of Lennard-Jones fluid [7, 8] and Lennard-Jones mixtures [9]. The Gibbs-Duhem integration was also utilized to calculate vapour–liquid equilibria for molecular model fluids and mixtures by molecular dynamics (MD) [10–12]. The Gibbs-Duhem integration combines the best elements of the GEMC technique and thermodynamic integration. The method, like the GEMC, entails simultaneous but independent simulations of each phase. The mechanism for equating the chemical potential is the Clapeyron equation. Hence, in contrast to the GEMC, no particle insertion is necessary. Starting at a state point for which the two phases are known to be in equilibrium, the Gibbs-Duhem integration method can be used to trace out the phase diagram directly and efficiently.

In this paper, we show how the Gibbs-Duhem integration can be applied to the SLE of molecular substances. As an example, we took the two-centre Lennard-Jones (2CLJ) system with elongation 0.67 for which vapour–liquid equilibria has already been determined [12, 13]. The elongation 0.67 corresponds to a halogenes-type of molecule. The next section describes the Clapeyron equation and its numerical solution by predictor–corrector methods. Section 3 gives the 2CLJ potential and simulation details. Section 4 predicts the starting solid–liquid coexistence point by the thermodynamic integration. Section 5 contains results of SLE obtained by the Gibbs-Duhem integration. Finally, we give conclusions in Section 6.

2 CLAPEYRON EQUATION

The Clapeyron equation [7] can be written in the Lennard-Jones reduced units (denoted by asterisk) [6] as

$$\left(\frac{d \ln p^*}{d(1/T^*)}\right)_\sigma = -\frac{T^*}{p^*}\frac{h_l^* - h_s^*}{1/\rho_l^* - 1/\rho_s^*} = f(1/T^*, p^*), \tag{1}$$

where p^* is the pressure, T^* is the temperature, h^*_l and h^*_s are the liquid and solid enthalpy, and ρ^*_l and ρ^*_s are the liquid and solid number density. The subscript σ indicates that the derivative is taken along the saturation line. Equation (1) is a first-order nonlinear differential equation that prescribes how the pressure must change with the temperature for liquid and solid phases to remain in coexistence.

Given an initial condition, *i.e.*, the pressure, temperature, $f(1/T^*, p^*)$, and equilibrium liquid and solid configuration at one coexistence point, Equation (1) can be solved numerically by a predictor–corrector method. We successfully applied the Adams predictor–corrector [7, 14]

$$\text{P} \quad y_{i+1} = y_i + \frac{\Delta\beta}{24}(55f_i - 59f_{i-1} + 37f_{i-2} - 9f_{i-3}) \tag{2}$$

$$\text{C} \quad y_{i+1} = y_i + \frac{\Delta\beta}{24}(9f_{i+1} + 19f_i - 5f_{i-1} + f_{i-2}) \tag{3}$$

to calculate the pressure. In Equations (2) and (3), y stands for $\ln p^*$, f for $f(1/T^*, p^*)$, P for the predictor, and C for the corrector; $\Delta\beta$ is the step in the $1/T^*$. The Adams algorithm requires four prior simulations. To perform the start-up, first, pressure at the first simulation point was predicted by the trapezoid predictor–corrector

$$\text{P} \quad y_1 = y_0 + \Delta\beta f_0 \tag{4}$$

$$\text{C} \quad y_1 = y_0 + \frac{\Delta\beta}{2}(f_1 + f_0). \tag{5}$$

Then, the midpoint predictor–corrector

$$\text{P} \quad y_2 = y_0 + 2\Delta\beta f_1 \tag{6}$$

$$\text{C} \quad y_2 = y_0 + \frac{\Delta\beta}{3}(f_2 + 4f_1 + f_0) \tag{7}$$

was used to determine the pressure at the second point. Finally, the midpoint predictor

$$y_3 = y_1 + 2\Delta\beta f_2 \tag{8}$$

with the Adams corrector

$$y_3 = y_2 + \frac{\Delta\beta}{24}(9f_3 + 19f_2 - 5f_1 + f_0) \tag{9}$$

was used to compute the pressure at the third point. The quantities needed to evaluate the right-hand side of the Clapeyron equation were obtained from simultaneous but independent constant pressure-constant temperature (NPT) MD simulations of the liquid and solid phases.

3 SIMULATION METHOD

3.1 Intermolecular Potential

The 2CLJ molecules consist of two interaction centres at a distance l apart which interact *via* the Lennard-Jones 12–6 potential. The 2CLJ potential, u_{2CLJ}, is

$$u_{2CLJ} = \sum_{a=1}^{2}\sum_{b=1}^{2} 4\varepsilon\left[\left(\frac{\sigma}{r_{ab}}\right)^{12} - \left(\frac{\sigma}{r_{ab}}\right)^{6}\right], \tag{10}$$

where r_{ab} is the distance between atom a of molecule i and atom b of molecule j, and ε and σ are the Lennard-Jones energy and size parameters.

3.2 Simulation Details

NPT MD simulations of the liquid phase were carried out using the Andersen method [6] and those of the solid phase were proceeded by the Parinello-Rahman method [15, 16]. The temperature was kept constant by the isokinetic scaling of translation and angular velocities after every time-step. The equations of translation and cell motions were solved by the Gear predictor–corrector algorithm of the fifth order. The rotational motion was treated by the method of quaternions, and it was also solved by the Gear predictor–corrector algorithm of the fifth order [6]. The minimum image convention, periodic boundary conditions, and a cut-off radius equal to (a) half-box length for liquid simulations and (b) 90% of minimum half-box length for solid simulations were used. The long-range correction of the potential energy, pressure and pressure tensor was included, assuming that

the radial distribution function is unity beyond the cut-off radius [6]. The membrane mass $M = 5 \cdot 10^{-4}$, the box mass $W = 2$, and the integration steps $\Delta t^* = 0.003$ for liquid simulations and $\Delta t^* = 0.001$ for solid simulations were used.

The free energy computations are necessarily carried out at a constant number of particles, volume and temperature, and a fixed box shape. This was easily achieved by the setting of membrane mass M and box mass W to large values. Thus, the cell motion was suppresed [6]. The box shape chosen for the free energy computations must be the equilibrium shape of the MD cell at the corresponding density [17].

During MD simulations, we also evaluated the diffusion coefficient D,

$$D = \lim_{t \to \infty} \frac{\delta(t)}{6t}, \tag{11}$$

where

$$\delta(t) = \langle |\mathbf{r}_i(t) - \mathbf{r}_i(0)|^2 \rangle, \tag{12}$$

the translation order parameter $\rho(k)$,

$$\rho(k) = \left\{ \left[\frac{1}{N} \sum_{i=1}^{N} \cos(\mathbf{k} \cdot \mathbf{r}_i) \right]^2 + \left[\frac{1}{N} \sum_{i=1}^{N} \sin(\mathbf{k} \cdot \mathbf{r}_i) \right]^2 \right\}^{1/2}, \tag{13}$$

and the rotational order parameter P_1,

$$P_1 = \frac{1}{N} \sum_{i=1}^{N} \mathbf{e}_i^{in} \cdot \mathbf{e}_i, \tag{14}$$

in order to obtain additional information on the development of the 2CLJ system with elongation 0.67. In Equations (11–14), t is the time, N is the number of molecules, $\mathbf{r}_i$ is the centre-of-mass position of molecule i, $\mathbf{k}$ is the reciprocal lattice vector of the initial lattice, and $\mathbf{e}_i^{in}$ and $\mathbf{e}_i$ are the unit vectors along molecular axis of molecule i in the initial and running configurations, respectively. If the limit (11) converges rapidly to a nonzero value, the system contains a fluid phase. The mobility of molecules in glassy or solid states is much lower and in such cases (11) converges slowly or not at all, while (12) fluctuates around a constant value describing a molecule

vibrating in a cage [18]. The translation order parameter is of order unity for a translation order structure, and positive and of order $1/\sqrt{N}$ for a translation disorder structure. Similarly, the rotational order parameter is of order unity for a rotational order structure and fluctuates around zero with amplitude $\mathcal{O}(1/\sqrt{N})$ when the structure is rotationally disordered [6].

4 STARTING SOLID–LIQUID COEXISTENCE POINT

Phase equilibrium requires that temperatures, pressure and chemical potential

$$\mu^* = f^* + \frac{p^*}{\rho^*}, \tag{15}$$

where f^* is the Helmholtz free energy, have to be the same in both regions. A solid–liquid coexistence point can be determined as the point of intersection of the solid and liquid isotherm branches in the $p^* - \mu^*$ plane [4]. Hence, determination of the solid–liquid coexistence point at a given temperature requires knowledge of the equation of state and free energy in both phases. Calculation of the equation of state and free energy for the 2CLJ system with elongation 0.67 was performed at $T^* = 1.45$, *i.e.*, at reduced temperature $T^*/T_C^* \sim 0.65$. Estimated critical parameters for this system [13] are $T_C^* = 2.3355$, $\rho_C^* = 0.17526$ and $p_C^* = 0.1367$.

4.1 Equation of State

4.1.1 Liquid

We carried out Andersen NPT MD simulations of liquid phase with 256 molecules in a cubic box for pressures up to $p^* = 80$. The simulation started at a low pressure (at a state point near the liquid coexistence curve), and then, higher pressures states were obtained by compression of the final configuration of a previous run. Starting configuration and pressure were the final configuration and pressure of a preliminary constant volume–constant temperature MD simulation. At each state point, the structure was allowed to relax 20000 timesteps from the final configuration of a previous simulation. The subsequent production run took 50000 timesteps. Table I summarizes results of liquid simulations. The equation of state is also shown in Figure 1.

TABLE I The equation of state for the two-centre Lennard-Jones system with elongation 0.67 in the liquid phase at reduced temperature 1.45. Pressures, number densities and internal energies are given in reduced units $p^* = p\sigma^3/\varepsilon$, $\rho^* = \rho\sigma^3$ and $u^* = U/N\varepsilon$, where N is the number of molecules, and ε and σ are the Lennard-Jones energy and size parameters. Deviations were calculated by dividing the whole simulation run into several blocks, each comprised of 1000 consecutive steps

	$T^* = 1.45$	
p^*	ρ^*	u^*
0.15	0.4593(19)	−11.46(5)
0.3	0.4652(18)	−11.61(5)
0.5	0.4720(16)	−11.77(5)
1.0	0.4862(15)	−12.11(5)
2.0	0.5076(12)	−12.59(4)
4.0	0.5377(8)	−13.16(3)
6.0	0.5598(8)	−13.49(3)
10.0	0.5930(6)	−13.82(3)
15.0	0.6231(6)	−13.88(3)
20.0	0.6467(6)	−13.73(3)
25.0	0.6659(5)	−13.43(3)
30.0	0.6832(8)	−13.09(5)
35.0	0.6984(10)	−12.70(6)
40.0	0.7115(8)	−12.21(5)
45.0	0.7241(7)	−11.74(3)
50.0	0.7340(5)	−11.12(3)
55.0	0.7443(4)	−10.57(2)
60.0	0.7532(3)	−9.95(1)
65.0	0.7620(1)	−9.30(1)
70.0	0.7697(2)	−8.66(1)
75.0	0.7770(1)	−7.99(1)
80.0	0.7839(1)	−7.31(1)

4.1.2 Solid

It is difficult or even impossible to establish a *priori* a stable structure of 2CLJ solids. Hence, we used as an initial configuration a close packed (CP) structure which tends to be the most stable, at least at very high pressure [19]. We chose the CP structure in which molecules of the 2CLJ solid with elongation 0.67 were stacked in layers parallel to the plane formed by **a** and **c** cell vectors. The molecules in the layer were arranged into triangular sequences with molecular axes parallel to each other. As in the CP structures used by Vega *et al.* [20] for hard dumbbells, we tilted molecular axes from the z direction by an angle equal to arcsin $(L/\sqrt{3})$, where $L = l/\sigma$ is the elongation. In the initial configuration, the **a** cell vector coincidented with the x Cartesian axis and the a, b plane laid in the x, y plane. The initial MD box contained 144 ($6 \times 6 \times 4$) molecules, and we set the ratio of cell lengths a: b: c equal to $6{:}6{:}4(1 + L)$.

We performed Parrinello-Rahmann NPT MD simulations for the CP solid, starting at pressure $p^* = 100$. Starting density was determined by trial and error in order to make the pressure at the first timestep roughly equal to the starting pressure $p^* = 100$. Then, lower pressures states were achieved by expansion of the final configuration of a previous run. As in the liquid simulation, at each state point, the structure was allowed to relax 40000 timesteps from the final configuration of a previous simulation. The length of the subsequent production run was 100000 timesteps. The CP structure remained mechanically stable with only a small change in the ratio of $a:b:c$ in respect to that of the initial CP structure, and with high translation and rotational order. The system was expanded until order parameters approached values typical for isotropic distribution, and the solid melted and jumped to the fluid branch. Table II presents results of solid simulations. The equation of state for the CP solid is also displayed in Figure 1. Figure 2 plots translation and rotational order parameters for the CP solid as a function of pressure.

It is important to note that the solid–liquid transition exhibits hysteresis [17]. The isotropic fluid can be overcompressed and the solid can be

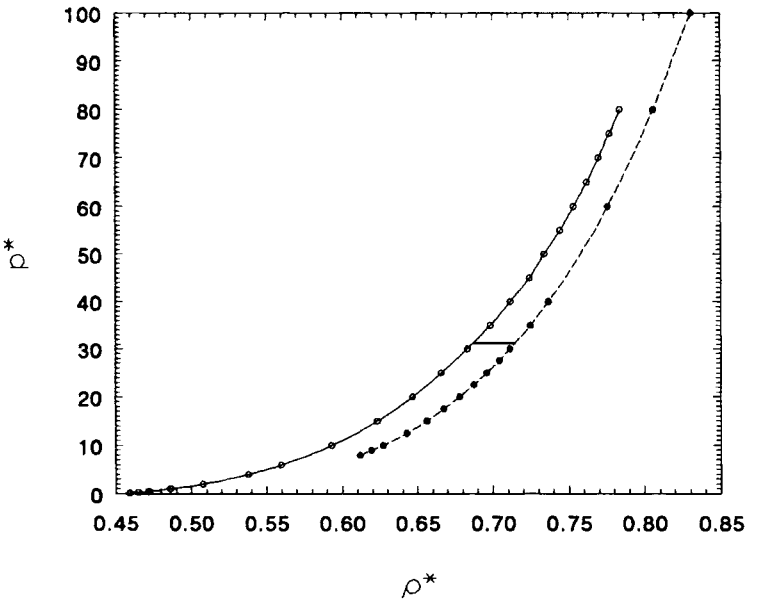

FIGURE 1 The equation of state for the two-centre Lennard-Jones system with elongation 0.67 at reduced temperature 1.45. The points are NPT MD simulation results and lines correspond to cubic spline fit.
(○, —: liquid; ●, - - -: close packed solid).

TABLE II The equation of state for the close-packed two-centre Lennard-Jones solid with elongation 0.67 at reduced temperature 1.45. Pressures, number densities and internal energies are given in reduced units $p^* = p\sigma^3/\varepsilon$, $\rho^* = \rho\sigma^3$ and $u^* = U/N\varepsilon$, where N is the number of molecules, and ε and σ are the Lennard-Jones energy and size parameters. Quantities a, b and c are the cell lengths, (**a**, **b**) is the angle between **a** and **b** cell vectors, (**a**, **c**) is the angle between **a** and **c** cell vectors, and (**b**, **c**) is the angle between **b** and **c** cell vectors. Deviations were calculated by dividing the whole simulation run into several blocks, each comprised of 1000 consecutive steps

p^*	ρ^*	u^*	a	b	c	(**a**, **b**)	(**a**, **c**)	(**b**, **c**)
100.0	0.8305(1)	−6.42(4)	5.926	5.940	6.131	59.99°	71.18°	73.73°
80.0	0.8059(1)	−9.16(1)	6.009	6.005	6.191	59.78°	70.95°	70.91°
60.0	0.7760(2)	−11.73(1)	6.096	6.092	6.301	59.79°	70.17°	69.95°
40.0	0.7367(2)	−13.93(1)	6.217	6.204	6.324	59.93°	71.01°	71.31°
35.0	0.7248(2)	−14.45(1)	6.248	6.251	6.342	59.93°	71.30°	71.19°
30.0	0.7113(3)	−14.89(1)	6.297	6.289	6.405	59.98°	70.40°	71.06°
27.5	0.7041(3)	−15.12(1)	6.321	6.319	6.439	59.91°	70.24°	70.37°
25.0	0.6961(3)	−15.30(1)	6.345	6.342	6.428	60.02°	70.47°	70.83°
22.5	0.6875(3)	−15.44(1)	6.373	6.376	6.451	60.00°	70.44°	71.02°
20.0	0.6781(4)	−15.56(2)	6.410	6.406	6.468	60.00°	70.90°	70.69°
17.5	0.6675(5)	−15.62(2)	6.448	6.451	6.510	59.95°	70.40°	70.45°
15.0	0.6561(6)	−15.69(2)	6.487	6.496	6.549	59.97°	70.22°	70.10°
12.5	0.6427(8)	−15.67(3)	6.547	6.541	6.564	59.97°	70.35°	70.47°
10.0	0.6270(10)	−15.55(4)	6.612	6.615	6.582	59.98°	70.46°	70.52°
9.0	0.6193(12)	−15.44(5)	6.646	6.648	6.603	60.02°	70.34°	70.31°
8.0	0.6116(15)	−15.35(7)	6.685	6.689	6.807	59.96°	67.29°	67.37°

overexpanded. Hysteresis effects are clearly visible in Figure 1. Thus, the solid–liquid coexistence point cannot be directly extracted from the equation of state.

4.2 Free Energy

The Helmholtz free energy at a density ρ^* is given by the thermodynamic integration [21] as

$$f^*(\rho^*) = f^*(\rho_1^*) + \int_{\rho_1^*}^{\rho^*} \frac{p^*}{\bar{\rho}^{*2}}\, d\bar{\rho}^*. \tag{16}$$

Equation (16) requires the knowledge of absolute free energy $f^*(\rho_1^*)$. It can be computed by thermodynamic integration as the free energy difference between convenient reference state (for which the free energy can be calculated analytically) and given state 1. To calculate this difference, a reversible path [21] is designed that transforms the potential between the reference and given system 1 at a constant number of particles, volume and

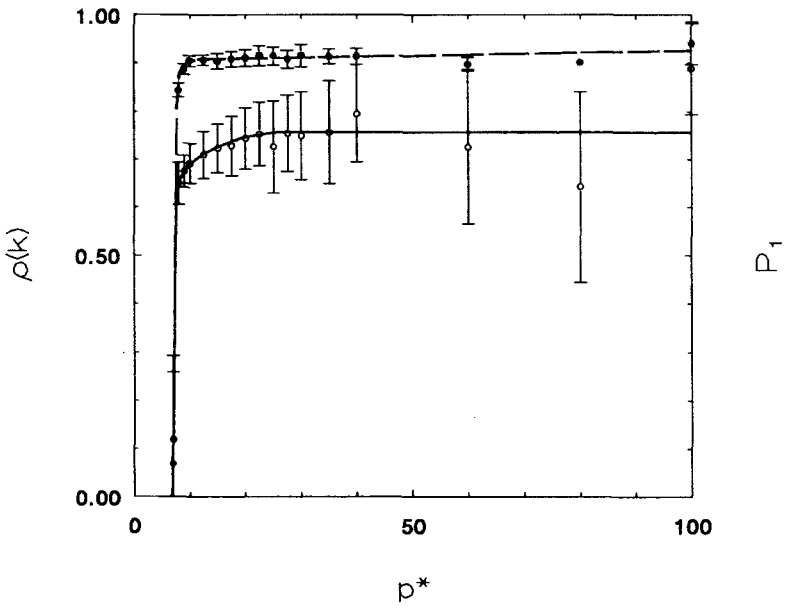

FIGURE 2 Translation order parameter $\rho(k)$ and rotational order parameter P_1 for the close-packed two-centre Lennard-Jones solid with elongation 0.67 as a function of pressure p^* (○, —: $\rho(k)$; ●, – – –: P_1). Lines are drawn only as a guide to the eye.

temperature, and a fixed box shape. Suppose that the transformation is a linear function of transformation parameter λ^k, where k is the integer and λ occurs in the range [0, 1]. The potential energy of the system U at a point of the transformation is

$$U(\lambda) = \lambda^k U_1 + (1 - \lambda^k) U_{\text{ref}}. \tag{17}$$

The free energy difference between the two states is given by the thermodynamic integration as

$$\Delta f^*(\rho_1^*) = \int_0^1 \left\langle \frac{\partial u^*(\lambda)}{\partial \lambda} \right\rangle_\lambda d\lambda = \int_0^1 k\lambda^{k-1} \langle u_1^* - u_{\text{ref}}^* \rangle_\lambda \, d\lambda, \tag{18}$$

where $\langle \cdot \rangle$ denotes an ensemble average. To calculate the free energy difference between the two systems, simulations at several values of λ are performed and the integral is calculated numerically.

4.2.1 *Liquid*

The absolute Helmholtz free energy was computed at $\rho_l^* = 0.46$. The liquid state ($\lambda = 1$) was changed continuously to the ideal gas (reference) state ($\lambda = 0$) by switching off the interaction potential proportionally to λ^4. The path was started from $\lambda = 1$, and each successive simulation at lower λ used a previous configuration as its starting point. At each λ point, the structure was equilibrated 20000 timesteps and subsequent production run took 50000 timesteps with the integration step $\Delta t^* = 0.003$. Pressure was always positive during transformation. For the numerical evaluation of the integral in Equation (18), we used 10-point Gauss-Legendre quadrature [14]. We also performed the free energy computations using the path from the ideal gas to liquid to prove that the integration path is reversible. Results of both free energy measurements were almost identical and are shown in Figure 3. Free energy of ideal gas, f_{ig}^*, (without a temperature-dependent constant that does not affect the phase equilibrium) is given as

$$f_{ig}^* \equiv f^*(\lambda = 0) = T^*(\ln \rho_l^* - 1), \tag{19}$$

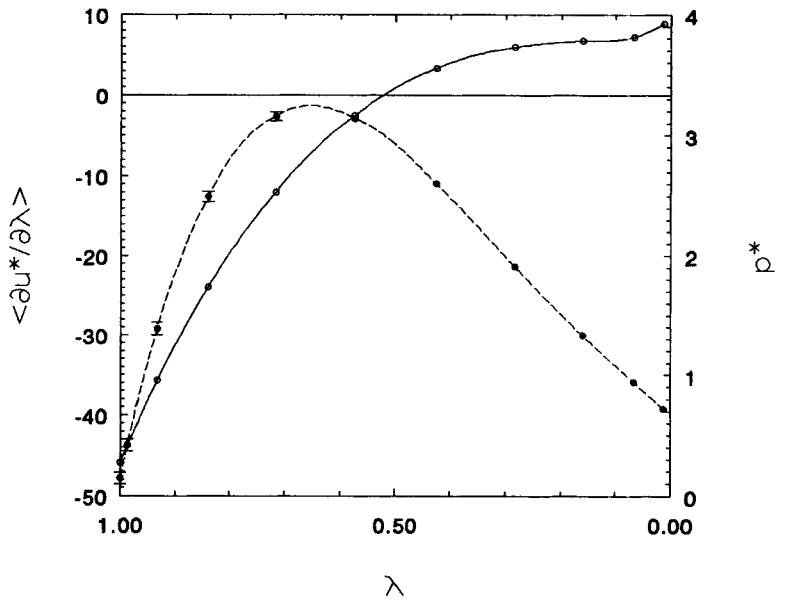

FIGURE 3 The integrand of equation (18) $\langle \partial u^*/\partial \lambda \rangle$ (○, —) and pressure p^* (●, – – –) as a function of transformation parameter λ during the transformation from the liquid to the ideal gas. Points are MD simulation results and lines correspond to cubic spline fit.

and has the value -2.576. The computed free energy difference between the liquid and ideal gas is $\Delta f^* = -5.879$. Kriebel *et al.* [13] calculated chemical potential for the 2CLJ system with elongation 0.67 by the Widom test particle insertion method [6] on the vapour–liquid coexistence curve. We used their value of chemical potential and the obtained equation of state, and calculated the absolute free energy at the state point considered, *i.e.*, at $T^* = 1.45$ and $\rho_1^* = 0.46$. We obtained the value $f^* = -8.52$, which is in excellent agreement with our value $f^* = -8.46$.

4.2.2 Solid

The absolute Helmholtz free energy was evaluated at $\rho_1^* = 0.8296$. A noninteracting Einstein crystal [17] was used as the reference system. The noninteracting Einstein crystal can be obtained by placing a solid in the strong external field

$$U_{\text{ref}} = \lambda_1 \sum_{i=1}^{N} (\mathbf{r}_i - \mathbf{r}_i^0)^2 + \lambda_2 \sum_{i=1}^{N} \sin^2 \alpha_i. \tag{20}$$

In Equation (20), λ_1 and λ_2 are large coupling constants, $\mathbf{r}_i - \mathbf{r}_i^0$ is the displacement of molecule i from its equilibrium position, and α_i is the angle between the axis of molecule i and the axis of molecule i in equilibrium position. Free energy of the noninteracting Einstein crystal, f_E^*, (without a temperature-dependent constant that does not affect the phase equilibrium) can be calculated analytically [20] as

$$f_E^* \equiv f^*(\lambda = 0) = -T^* \ln [J(\lambda_2^*)] - \frac{T^*}{N} \ln \left[N^{-3/2} \left(\frac{\pi}{\lambda_1^*} \right)^{3(N-1)/2} \right], \tag{21}$$

where

$$\ln [J(\lambda_2^*)] = \int_0^1 \exp [\lambda_2^* (x^2 - 1)] \, dx, \tag{22}$$

$\lambda_1^* = \lambda_1/(k_B T/\sigma^2)$ and $\lambda_2^* = \lambda_2/(k_B T)$; with k_B denoting the Boltzmann constant. The coupling constants were chosen to have the same values in reduced units, *i.e.*, $\lambda_1^* = \lambda_2^* = \lambda^*$ and we used $\lambda^* = 8000$. The free energy of the noninteracting molecular Einstein crystal is $f_E^* = 30.38$.

The solid was transformed from the 'realistic' crystal ($\lambda = 1$) to the noninteracting Einstein crystal ($\lambda = 0$) in 19 discrete steps by switching off the interaction potential proportionally to λ^2 and switching on the external

field proportionally to $(1-\lambda^2)$. The starting configuration for each simulation was a final configuration produced at a previous, higher, λ value. Typically at each λ point, the structure was equilibrated 40000 timesteps, and the following production run took 200000 timesteps with integration step $\Delta t^* = 0.00025$. Transformation was then reversed to reproduce the 'realistic' crystal. Results of both free energy measurements were nearly identical and are plotted in Figure 4. We fitted the integrand in Equation (18) to cubic spline and evaluated the integral in Equation (18) by Simpson's rule. The calculated free energy difference between the solid and noninteracting Einstein crystal is $\Delta f^* = -19.73$, and the absolute free energy at the state point considered, *i.e.*, at $T^* = 1.45$ and $\rho_1^* = 0.8296$ is $f^* = 10.64$.

The intersection of solid and liquid isotherm branches in the pressure *vs* chemical potential plane is at $p^* = 31.211$ and $\mu^* = 42.950$. Thus, the starting solid–liquid coexistence point at $T^* = 1.45$ has the following parameters: $p_\sigma^* = 31.211$, $\rho_l^* = 0.6870(6)$, $\rho_s^* = 0.7148(2)$, $h_l^* = 36.05(7)$ and $h_s^* = 32.47(5)$.

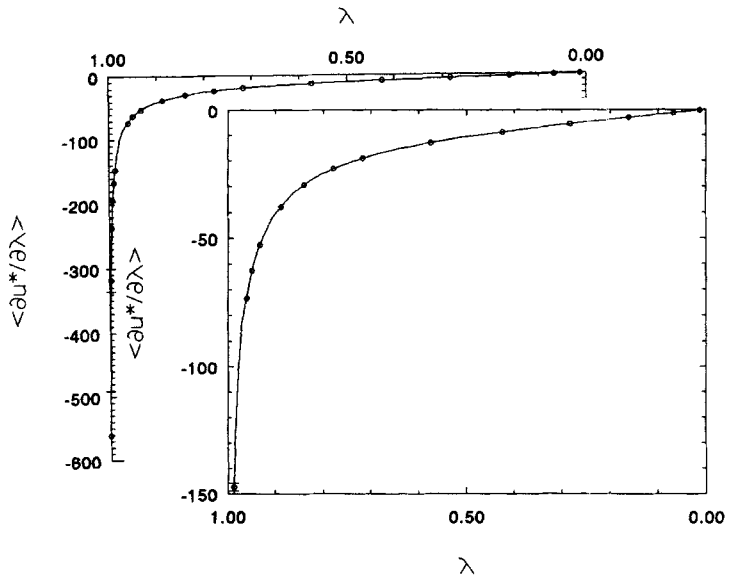

FIGURE 4 The integrand of equation (18) $\langle \partial u^*/\partial\lambda \rangle$ (○: MD simulations, —: cubic spline fit) as a function of transformation parameter λ during the transformation from the close-packed solid to the noninteracting Einstein crystal.

5 SOLID–LIQUID EQUILIBRIA BY GIBBS-DUHEM INTEGRATION

The Gibbs-Duhem integrations were performed for the 2CLJ system with elongation 0.67 between temperatures 1.45–3.86, and 1.45-triple temperature. We proceeded with the Gibbs-Duhem integration method in the following manner. Starting from the solid–liquid coexistence point at $T^* = 1.45$, the temperature was increased (decreased) and the predictor pressure was calculated according to Equation (4). Afterwards, the liquid and solid configurations were allowed to relax by 20000 and 40000 timesteps, respectively. At the end of the relaxation period, all accumulators were set to zero. The subsequent production run of the liquid and solid phases was divided into two timeblocks. The timeblocks contained 25000 and 50000 timesteps each for the liquid and the solid phase, respectively. After each timeblock was completed, the computed running averages of liquid and solid number density, and liquid and solid enthalpy, were used to evaluate the right-hand side of the Clapeyron equation, and thus, to calculate the corrector pressure according to Equation (5). Then, the temperature was again increased (decreased) and the process was repeated. The predictor and corrector pressures were evaluated according to appropriate equations: Equations (2,3 and 6–9). The reciprocal temperature $1/T^*$ was increased (decreased) in constant steps $\Delta\beta$ of 0.0012 (0.016). At each temperature, the NPT MD simulations of the liquid and solid phase were carried out simultaneously but independently, using Andersen and Parinello-Rahmann algorithms, respectively.

Results of SLE obtained by the Gibbs-Duhem integration for the 2CLJ system with elongation 0.67 are listed in Table III for selected temperatures. Figure 5 shows the solid–liquid coexistence pressure as a function of temperature, and Figure 6 displays the phase diagram. Vapour–liquid equilibria data for the 2CLJ system with elongation 0.67 were taken from Kriebel *et al.* [13]. Triple temperature $T_t^* \approx 0.62$ was estimated as the temperature where the solid–liquid coexistence pressure determined by the Gibbs-Duhem integration was zero. The ratio of T_t^*/T_C^* is about 0.27 and the triple number density has the value $\rho_t^* \approx 0.573$. The density jump at freezing is about 7.2% at the triple temperature, that is, about 3.6% at the critical temperature, and is about 3.3% at $T^* = 1.65\,T_C^*$.

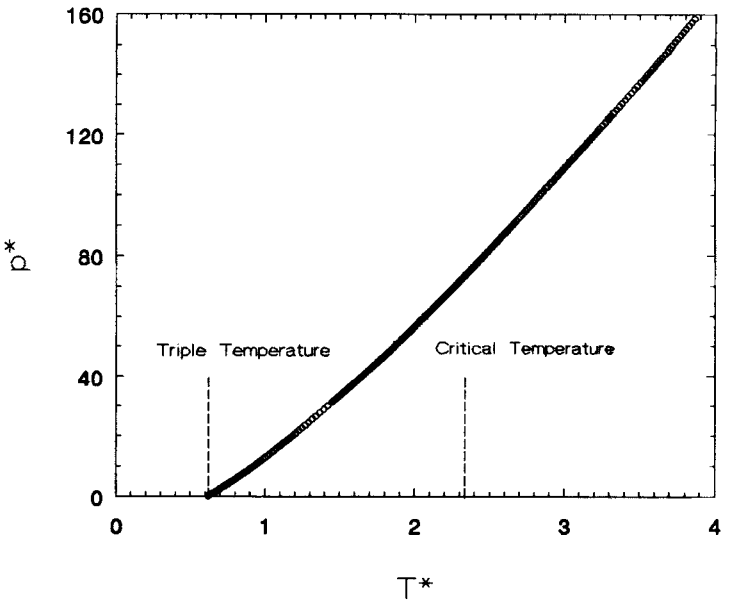

FIGURE 5 Solid–liquid coexistence pressure p_z^* as a function of temperature T^* for the two-centre Lennard-Jones system with elongation 0.67 (○: the Gibbs-Duhem integration).

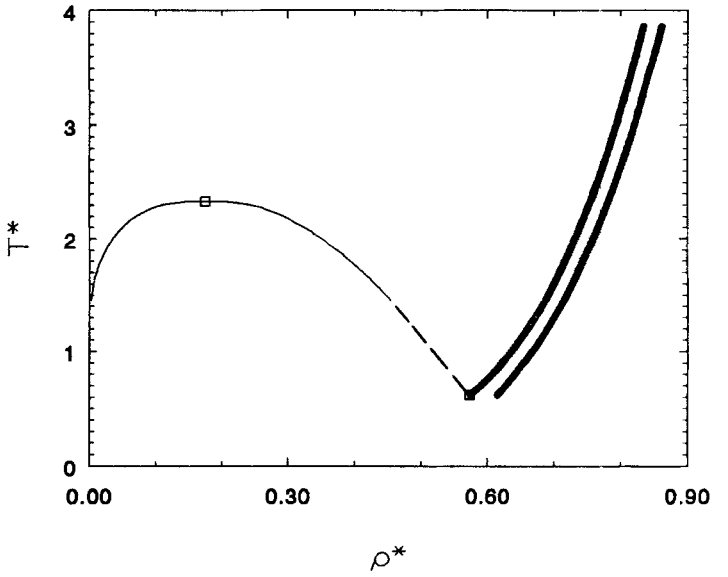

FIGURE 6 Phase diagram for the two-centre Lennard-Jones system with elongation 0.67 (—: vapour–liquid coexistence lines [13]; – – –: extrapolation of liquid coexistence line; ○: liquid (fluid) coexistence line by the Gibbs-Duhem integration; ●: solid coexistence line by the Gibbs-Duhem integration). The estimated critical [13] and triple points are indicated by squares.

TABLE III Solid–liquid equilibria for the two-centre Lennard-Jones system with elongation 0.67. Temperatures, pressures, number densities and internal energies are given in reduced units $T^* = k_B T/\varepsilon$, $p^* = p\sigma^3/\varepsilon$, $\rho^* = \rho\sigma^3$ and $u^* = U/N\varepsilon$, where N is the number of molecules, k_B is the Boltzmann constant, and ε and σ are the Lennard-Jones energy and size parameters. Subscripts l and s denote liquid and solid, respectively. Quantities a, b and c are the cell lengths, (**a**, **b**) is the angle between **a** and **b** cell vectors, (**a**, **c**) is the angle between **a** and **c** cell vectors, and (**b**, **c**) is the angle between **b** and **c** cell vectors. Deviations were calculated by dividing the whole simulation run into several blocks, each comprised of 1000 consecutive steps

T^*	p_σ^*	ρ_l^*	ρ_s^*	u_l^*	u_s^*	a	b	c	(**a**, **b**)	(**a**, **c**)	(**b**, **c**)
0.6207	0.160	0.5735(9)	0.6148(4)	−15.51(4)	−17.52(2)	6.64	6.64	6.65	59.9°	70.8°	70.7°
0.7013	2.547	0.5900(8)	0.6273(4)	−15.58(3)	−17.48(2)	6.59	6.59	6.60	59.9°	70.9°	71.0°
0.8060	5.869	0.6082(9)	0.6419(4)	−15.50(4)	−17.26(2)	6.54	6.54	6.57	59.9°	71.0°	70.7°
0.9479	10.80	0.6292(10)	0.6619(3)	−15.19(5)	−17.10(1)	6.46	6.47	6.54	59.9°	70.5°	70.4°
1.094	16.40	0.6490(8)	0.6791(3)	−14.71(4)	−16.54(1)	6.41	6.40	6.48	59.9°	70.6°	70.7°
1.205	20.86	0.6619(8)	0.6911(3)	−14.24(4)	−16.05(2)	6.36	6.36	6.43	60.0°	70.9°	71.1°
1.316	25.48	0.6736(6)	0.7023(3)	−13.70(4)	−15.49(1)	6.32	6.32	6.43	60.0°	70.4°	70.7°
1.450	31.21	0.6870(6)	0.7148(3)	−13.00(3)	−14.79(1)	6.29	6.27	6.39	60.0°	70.6°	71.1°
1.552	35.68	0.6963(6)	0.7238(3)	−12.43(4)	−14.21(1)	6.25	6.26	6.39	59.9°	70.3°	70.5°
1.650	40.04	0.7044(6)	0.7317(3)	−11.82(4)	−13.60(2)	6.23	6.23	6.37	60.0°	70.4°	70.4°
1.772	45.58	0.7143(6)	0.7411(3)	−11.05(5)	−12.83(3)	6.20	6.20	6.36	60.0°	70.5°	70.2°
1.875	50.34	0.7222(8)	0.7489(3)	−10.39(5)	−12.19(2)	6.17	6.17	6.32	60.0°	70.7°	70.7°
1.983	55.59	0.7302(8)	0.7575(3)	−9.614(54)	−11.65(3)	6.15	6.14	6.30	60.0°	70.8°	71.0°
2.105	61.64	0.7390(7)	0.7661(2)	−8.741(44)	−10.79(2)	6.12	6.13	6.29	59.9°	70.8°	70.3°
2.251	69.05	0.7491(6)	0.7760(2)	−7.657(42)	−9.773(16)	6.09	6.10	6.25	59.8°	70.8°	71.2°
2.407	77.09	0.7593(6)	0.7860(2)	−6.455(54)	−8.599(15)	6.06	6.06	6.23	60.0°	70.8°	71.5°
2.509	82.44	0.7653(8)	0.7923(2)	−5.615(68)	−7.805(25)	6.05	6.05	6.23	59.9°	70.6°	70.7°
2.608	87.71	0.7711(9)	0.7981(2)	−4.784(78)	−7.036(13)	6.03	6.03	6.21	59.9°	71.0°	70.7°
2.703	92.81	0.7766(8)	0.8036(2)	−4.014(72)	−6.275(18)	6.02	6.01	6.19	59.9°	70.8°	71.2°

2.806	98.35	0.7825(7)	0.8091(3)	−3.179(62)	−5.395(37)	5.99	6.00	6.16	60.0°	71.6°	71.6°
2.902	103.6	0.7875(7)	0.8144(2)	−2.355(71)	−4.625(34)	5.98	5.99	6.22	60.0°	70.5°	70.2°
3.005	109.3	0.7934(8)	0.8198(2)	−1.520(81)	−3.786(18)	5.97	5.97	6.20	59.8°	70.4°	70.1°
3.100	114.5	0.7977(7)	0.8246(2)	−0.636(70)	−2.995(19)	5.96	5.96	6.15	59.8°	70.9°	71.2°
3.201	120.1	0.8029(9)	0.8296(2)	0.188(86)	−2.126(26)	5.94	5.94	6.14	59.9°	71.4°	71.0°
3.308	126.2	0.8083(9)	0.8348(2)	1.141(74)	−1.209(38)	5.93	5.92	6.14	60.0°	70.7°	71.2°
3.403	131.5	0.8128(7)	0.8392(2)	2.003(73)	−0.357(30)	5.92	5.91	6.11	59.9°	71.4°	71.3°
3.504	137.3	0.8171(7)	0.8439(2)	2.924(61)	0.525(45)	5.90	5.90	6.11	60.0°	71.4°	71.2°
3.599	142.9	0.8217(7)	0.8490(2)	3.781(79)	1.010(31)	5.90	5.87	6.09	60.1°	72.1°	71.1°
3.699	148.9	0.8262(7)	0.8537(2)	4.741(68)	1.940(47)	5.89	5.88	6.14	59.8°	70.6°	70.5°
3.804	155.3	0.8310(8)	0.8586(2)	5.723(84)	2.866(37)	5.87	5.86	6.12	59.9°	70.7°	71.0°
3.860	158.6	0.8337(9)	0.8610(2)	6.241(85)	3.376(38)	5.86	5.86	6.08	60.0°	71.3°	71.5°

6 CONCLUSIONS

We directly evaluated the solid–liquid equilibria by MD simulations using the Gibbs-Duhem integration method [7]. The Gibbs-Duhem integration method, like the GEMC, performed simultaneous but independent simulations of each phase. However, in contrast to the GEMC, the Gibbs-Duhem integration does not require particle insertion. The Gibbs-Duhem integration method was applied to the 2CLJ system with elongation 0.67. The necessary initial coexistence point for initiation of the Gibbs-Duhem integration was determined as the point of intersection of solid and liquid isotherm branches in the pressure *vs* chemical potential plane. Solid–liquid equilibria for the 2CLJ system with elongation 0.67 was determined between triple temperature and 1.65 times critical temperature. Ratio of triple to critical temperature was estimated to be about 0.27 and that of triple to critical number density to be about 3.27.

Acknowledgement

ML would like to acknowledge the partial support of the Grant Agency of the Academy of Sciences of the Czech Republic, grant No. 472401. Calculations were made on the IBM SP2 in the Joint Computer Center of Czech Technical University, Institute of Chemical Technology and IBM Czech Republic, Prague. Authors would like to thank Prof. C. Machann for a careful reading of the manuscript.

References

[1] Hansen, J.-P. and Verlet, L. (1969). "Phase transitions of the Lennard-Jones system", *Phys. Rev.*, **184**, 151–161.
[2] Meijer, E. J., Frenkel, D., LeSar, R. A. and Ladd, A. J. C. (1990). "Location of melting point at 300 K of nitrogen by Monte Carlo simulation", *J. of Chem. Phys.*, **92**, 7570–7575.
[3] Báez, L. A. and Glancy, P. (1995). "Phase equilibria in extended simple point charge ice-water systems", *J. of Chem. Phys.*, **103**, 9744–9755.
[4] Möller, D. and Fischer, J. (1994). "Determination of an effective intermolecular potential for carbon dioxide using vapour–liquid phase equilibria from NpT + test particle simulations", *Fl. Ph. Eq.*, **100**, 35–61.
[5] Panagiotopoulos, A. Z. (1992). "Direct determination of fluid phase equilibria by simulation in the Gibbs ensemble: A review", *Mol. Sim.*, **9**, 1–23.
[6] Allen, M. P. and Tildesley, D. J. (1987). *Computer Simulation of Liquids*, Oxford: Clarendon Press.
[7] Kofke, D. A. (1993). "Direct evaluation of phase coexistence by molecular simulation via integration along saturation line", *J. Chem. Phys.*, **98**, 4149–4162.
[8] Kofke, D. A. (1993). "Gibbs-Duhem integration: A new method for direct evaluation of phase coexistence by molecular simulation", *Mol. Phys.*, **78**, 1331–1336.

[9] Mehta, M. and Kofke, D. A. (1994). "Coexistence diagrams of mixtures by molecular simulation", *Chem. Eng. Sci.*, **49**, 2633–2645.
[10] Lísal, M. and Vacek, V. (1996). "Direct evaluation of vapour–liquid equilibria by molecular dynamics using Gibbs-Duhem integration", *Mol. Sim.*, **17**, 27–39.
[11] Lísal, M. and Vacek, V. (1996). "Direct evaluation of vapour–liquid equilibria of mixtures by molecular dynamics using Gibbs-Duhem integration", *Mol. Sim.*, **18**, 75–99.
[12] Lísal, M., Budinský, R. and Vacek, V. (1996). "Vapour–liquid equilibria for dipolar two-centre Lennard-Jones fluids by Gibbs-Duhem integration", *Fl. Ph. Eq.*, submitted.
[13] Kriebel, Ch., Müller, A., Winkelmann, J. and Fischer, J. (1995). "Vapour–liquid equilibria of two-centre Lennard-Jones fluids from the NpT plus test particle method", *Mol. Phys.*, **84**, 381–394.
[14] Press, W. H., Flannery, B. P., Teukolsky, S. A. and Vetterling, W. T. (1989). *Numerical Recipes*, New York: Cambridge University Press.
[15] Parrinello, M. and Rahman, A. (1980). "Crystal structure and pair potentials: A molecular-dynamics study", *Phys. Rev. Lett.*, **45**, 1196–1199.
[16] Nosé, S. and Klein, M. L. (1983). "A study of solid and liquid carbon tetrafluoride using the constant pressure molecular dynamics technique", *J. of Chem. Phys.*, **78**, 6928–6939.
[17] Frenkel, D. and Mulder, B. M. (1985). "The hard ellipsoid-of-revolution fluid. I. Monte Carlo simulations", *Mol. Phys.*, **55**, 1171–1192.
[18] Nezbeda, I. and Kolafa, J. (1995). "The use of control quantities in computer simulation experiments: Application to the exp-6 potential fluid", *Mol. Sim.*, **15**, 153.
[19] Kitaigorodsky, A. I. (1973). *Molecular crystals and molecules*, New York: Academic Press.
[20] Vega, C., Paras, E. P. A. and Monson, P. A. "Solid–fluid equilibria for hard dumbbells via Monte Carlo simulation", *J. of Chem. Phys.*, **96**, 9060–9072.
[21] Frenkel, D. (1985). in *Molecular Dynamics Simulation of Statistical-Mechanical Systems*, International School of Physics "Enrico Fermi", Course No. XCVII, edited by G. Ciccotti and W. G. Hoover, Amsterdam: North-Holland.